

UC San Diego

UC San Diego Previously Published Works

Title

RNA-binding protein RBM3 intrinsically suppresses lung innate lymphoid cell activation and inflammation partially through CysLT1R

Permalink

<https://escholarship.org/uc/item/2jc7f62m>

Journal

Nature Communications, 13(1)

ISSN

2041-1723

Authors

Badrani, Jana H
Strohm, Allyssa N
Lacasa, Lee
[et al.](#)

Publication Date

2022

DOI

10.1038/s41467-022-32176-5

Peer reviewed

RNA-binding protein RBM3 intrinsically suppresses lung innate lymphoid cell activation and inflammation partially through CysLT1R

Received: 17 July 2020

Accepted: 19 July 2022

Published online: 30 July 2022

 Check for updates

Jana H. Badrani¹, Allyssa N. Strohm^{1,2}, Lee Lacasa¹, Blake Civello¹, Kellen Cavagnero¹, Yung-An Haung^{1,3}, Michael Amadeo¹, Luay H. Najji¹, Sean J. Lund¹, Anthea Leng¹, Hyojoung Kim¹, Rachel E. Baum¹, Naseem Khorram¹, Monalisa Mondal⁴, Grégory Seumois⁴, Julie Pilotte⁵, Peter W. Vanderklish⁵, Heather M. McGee^{1,6,7,8} & Taylor A. Doherty^{1,2} ✉

Innate lymphoid cells (ILC) promote lung inflammation in asthma through cytokine production. RNA-binding proteins (RBPs) are critical post-transcriptional regulators, although less is known about RBPs in ILC biology. Here, we demonstrate that RNA-binding motif 3 (RBM3) is highly expressed in lung ILCs and is further induced by alarmins TSLP and IL-33. *Rbm3*^{-/-} and *Rbm3*^{-/-}*Rag2*^{-/-} mice exposed to asthma-associated *Alternaria* allergen develop enhanced eosinophilic lung inflammation and ILC activation. IL-33 stimulation studies in vivo and in vitro show that RBM3 suppressed lung ILC responses. Further, *Rbm3*^{-/-} ILCs from bone marrow chimeric mice display increased ILC cytokine production suggesting an ILC-intrinsic suppressive function of RBM3. RNA-sequencing of *Rbm3*^{-/-} lung ILCs demonstrates increased expression of type 2/17 cytokines and cysteinyl leukotriene 1 receptor (CysLT1R). Finally, *Rbm3*^{-/-}*Cyslt1r*^{-/-} mice show dependence on CysLT1R for accumulation of ST2⁺IL-17⁺ ILCs. Thus, RBM3 intrinsically regulates lung ILCs during allergen-induced type 2 inflammation that is partially dependent on CysLT1R.

Lung innate lymphoid cells (ILC) are critical players in inflammatory diseases including helminth infections, asthma, and pulmonary fibrosis¹⁻⁴. Once activated by epithelial cytokines, such as TSLP, IL-33, IL-25, and lipid mediators including leukotrienes, group 2 innate lymphoid cells (ILC2) produce type 2 cytokines IL-4, IL-5, IL-9, and IL-13^{5,6}. These cytokines are major contributors to the characteristics of type 2 asthma such as airway inflammation, hyperresponsiveness, and remodeling. IL-13 promotes mucus production and

airway hyperresponsiveness, IL-4 regulates IgE synthesis and Th2 cell differentiation, and IL-5 controls the survival and activation of eosinophils^{7,8}. In addition to the contribution of ILC2s in asthma, there is also evidence that IL-17A production by “inflammatory” iILC2s (or ILC2-17s) as well as ILC3s promote lung inflammatory responses in asthma models^{2,9,10}. For example, cysteinyl leukotrienes induce IL-17A from ST2⁺ lung ILC2s and transferred IL-17^{-/-} ILC2s are less pathogenic during type 2 lung inflammation¹⁰. Since

¹Division of Rheumatology, Allergy and Immunology, Department of Medicine, University of California San Diego, La Jolla, CA, USA. ²Veterans Affairs San Diego Health Care System, La Jolla, CA, USA. ³Department of Microbiology and Immunology, College of Medicine, Chang Gung University, Taoyuan, Taiwan. ⁴La Jolla Institute, La Jolla, CA, USA. ⁵The Scripps Research Institute, La Jolla, CA, USA. ⁶NOMIS Center for Immunobiology and Microbial Pathogenesis, Salk Institute, La Jolla, CA, USA. ⁷Departments of Radiation Oncology and Immuno-Oncology, City of Hope, Duarte, CA, USA. ⁸Department of Molecular Medicine, La Jolla, CA, USA. ✉e-mail: tdoherty@ucsd.edu

the discovery of ILCs, most studies have focused on mechanisms of ILC activation, and there are fewer reports that provide insights into suppression of ILC responses. Modulation of ILC2s may occur through individual cytokines^{11,12} and lipid mediators, and cell-cell contact pathways^{13,14}. Interestingly, despite the known regulatory activity of microRNAs (miRNAs) in post-transcriptional repression, studies have demonstrated that miR-19 and miR-155 promote ILC2 activation and survival^{15,16}. Overall, our understanding of mechanisms that broadly suppress both type 2 and 17 cytokine production in lung ILCs is limited.

Regulation of immune cell responses occurs through gene expression as well as post-transcriptional and post-translational pathways. RNA-binding proteins (RBPs) regulate cellular responses via stabilization or degradation of mRNA transcripts as well as effects on miRNA processing¹⁷. The RBP HuR stabilizes target mRNAs including *gata3* transcripts in CD4⁺ Th2 cells through binding to AU-rich element (ARE) sequences in the 3'UTR¹⁸. AREs are also present in Th2-cytokine transcripts including *Il4*, *Il5*, *Il13*, and therefore are potential post-transcriptional regulatory targets for RBPs¹⁹. Very recently, naïve ILC2s were shown to express the RBP tristetraprolin (TTP) which inhibits Th2 cytokine production and is downregulated after IL-33 stimulation²⁰. Aside from these studies, how RBPs control ILC responses is not well explored and likely represents an important level of ILC regulation in inflammatory diseases.

In this work, we perform RNA sequencing of purified lung ILC subsets from fungal allergen-challenged mice based on CD127 and ST2²¹ and assess levels of RBP transcripts in ILC subsets. The *Rbm3* transcript which encodes RNA-binding motif 3 (RBM3) is one of the most highly expressed RBPs in ILCs, second to *Zfp36* (encodes TTP)²⁰, and with a higher expression level than *Elavl1*, which encodes for HuR. RBM3 is a cold shock protein that has been demonstrated to enhance the stability and translation of mRNAs for COX-2, IL-8, and VEGF²². Further, RBM3 interacts with microRNAs miR-142-5p and miR-143, temperature-sensitive microRNAs implicated in the fever response²³, as well as with the RBP HuR²². Using fungal allergen-driven and IL-33-driven lung inflammation models with *Rbm3*^{-/-}, *Rbm3*^{-/-}*Rag2*^{-/-}, and *Rbm3*^{-/-}*Cyslt1r*^{-/-} mice, as well as in vitro studies, mixed bone marrow chimera studies, and transcriptomic analysis, we show that RBM3 negatively regulates lung ILC type 2 and 17 cytokine responses that are partially dependent on CysLT1R signaling. Contrary to previous reports showing stabilization of cytokine transcripts by RBM3, the data presented herein demonstrates that RBM3 suppresses ILC2 activation in the lung.

Results

RBM3 is highly expressed among RNA-binding protein mRNAs in activated lung ILCs

ILC subtypes can be defined by expression of CD127 (IL-7R) and ST2 (IL-33R) and we recently showed that single negative or double negative “unconventional” subpopulations for these markers include heterogeneous ILC populations that express GATA-3 and produce type 2 cytokines²¹. Upon airway challenge with the asthma-associated fungal allergen *Alternaria alternata*, all four Thy1.2⁺ subpopulations (CD127⁺ST2⁻, CD127⁺ST2⁺, CD127⁻ST2⁺, and CD127⁻ST2⁻) are activated. Lin⁻Thy1.2⁺ lymphocytes from WT mice challenged over 10 days with 50 µg *Alternaria* were FACS purified based on expression of CD127 and ST2 (Supplementary Fig. 1a). Next, we performed RNA-Seq analysis and detected 207 RNA-binding protein (RBPs) transcripts expressed by the ILC subpopulations (Supplementary Fig. 1b). Of the top 25 differentially expressed RBPs (Fig. 1a), *Zfp36*, which encodes for tristetraprolin (TTP), was the most highly expressed RBP. *Zfp36*^{-/-} mice develop spontaneous prominent inflammation and severe autoimmune disease²⁴, and a very recent report demonstrates that TTP regulates ILC2 homeostasis²⁰. After *Zfp36*, *Rbm3* was the next highest RBP with transcript levels increased over *Elavl1*, which encodes for HuR (Fig. 1b)

which has been shown to promote GATA-3 expression and type 2 cytokines in T cells^{18,25}. Since we were interested in RBP function using in vivo asthma models, we focused on regulation by RBM3 given that *Rbm3*^{-/-} mice are viable and not known to spontaneously have immune disease^{25,26}. Sorted Thy1.2⁺ lung ILCs from *Alternaria*-challenged mice expressed *Rbm3* mRNA at levels on par with *Il5* mRNA though less than *Gata3*, *Rora*, and *Il13* (Fig. 1c). qPCR analysis of the four ILC populations based on ST2 and CD127 showed that *Rbm3* expression was highest in ST2⁺ ILCs that also more highly expressed *Cyslt1r*, *Il5*, *Il13*, and *Il17* (Supplementary Fig. 2). Thus, of 207 RBP transcripts from in vivo activated lung ILCs, *Rbm3* was expressed at levels comparable to molecules involved in ILC function and thus is a candidate protein that might regulate ILC function and lung inflammation.

Alternaria, IL-33, and TSLP increase lung and ILC RBM3 expression

To ascertain whether RBM3 is induced during type 2 inflammation, *Alternaria*-challenged mice were assessed for RBM3 levels by immunostaining. Increased expression of RBM3 was detected by immunofluorescence in *Alternaria*-challenged lungs compared to naïve control lungs (Supplementary Fig. 3a). RBM3 expression was visualized in epithelial as well as subepithelial cells which was further induced by challenge with *Alternaria*. As ILCs regulate innate lung responses to *Alternaria*²⁶, we investigated changes in RBM3 levels in lung ILCs. Lin⁻Thy1.2⁺ ILCs from the lungs of challenged mice demonstrated increased RBM3 expression by intracellular flow cytometry when compared to naïve and PBS-challenged controls (Fig. 1d). Interestingly, eosinophils and macrophages analyzed from challenged mice did not show increases in RBM3 expression (Supplementary Fig. 3b).

As IL-33 and TSLP are critical epithelial cytokines that regulate ILC2 responses, we assessed levels of RBM3 in *Tslpr*^{-/-} mice and WT mice treated with IL-33 blocking antibody. RBM3 expression in *Tslpr*^{-/-} mice and WT mice receiving anti-IL-33R was reduced compared with controls (Fig. 1e). We next assessed whether human ILC2s expressed RBM3 and if TSLP and IL-33 regulated RBM3 expression as they do in mouse ILCs. FACS purified human ILC2s stimulated with a combination of TSLP and IL-33 demonstrated significantly increased RBM3 immunostaining after 24 h and 72 h compared with control staining (Supplementary Fig. 4). Thus, activation of ILCs by epithelial cytokines IL-33 and TSLP led to increased RBM3 expression in both mice and humans, suggesting studies of RBM3 in mouse ILCs might be relevant to humans.

RBM3 suppresses *Alternaria*-induced type 2 lung inflammation

We next performed in vivo asthma model experiments with *Rbm3*^{-/-} mice to assess lung inflammatory and ILC responses. We analyzed lineage-negative Thy1.2⁺ lung ILCs from naïve *Rbm3*^{-/-} mice and found no significant changes in the absolute or relative number of ILCs between naïve WT and *Rbm3*^{-/-} mice (Supplementary Fig. 5a, b). Naïve *Rbm3*^{-/-} ILCs had similar surface marker expression of common ILC2 surface markers when compared to WT ILC2s (Supplementary Fig. 5c), and naïve *Rbm3*^{-/-} mice also showed similar levels of BAL and lung eosinophils as WT controls (Supplementary Fig. 5d, e). Thus, *Rbm3*^{-/-} mice are phenotypically similar to WT mice in terms of baseline lung eosinophil and ILC levels.

To ascertain potential effects of RBM3 in vivo, we repetitively challenged WT and *Rbm3*^{-/-} mice with *Alternaria*, a fungal allergen that induces potent type 2 lung inflammation and ILC activation^{21,26,27}. *Rbm3*^{-/-} mice challenged with *Alternaria* three times over 7 days developed significant increases in BAL and lung eosinophils (Siglec-F⁺CD11c⁻ cells) and neutrophils (Siglec-F⁻GR-1⁺ cells) compared to WT mice (Fig. 2a, b). Similarly, *Rbm3*^{-/-} mice receiving 4 challenges over 10 days also showed increased eosinophils and neutrophils in BAL and lung (Fig. 2c, d) as well as increased BAL levels of IL-5 and IL-13 (Fig. 2e). Further, lung

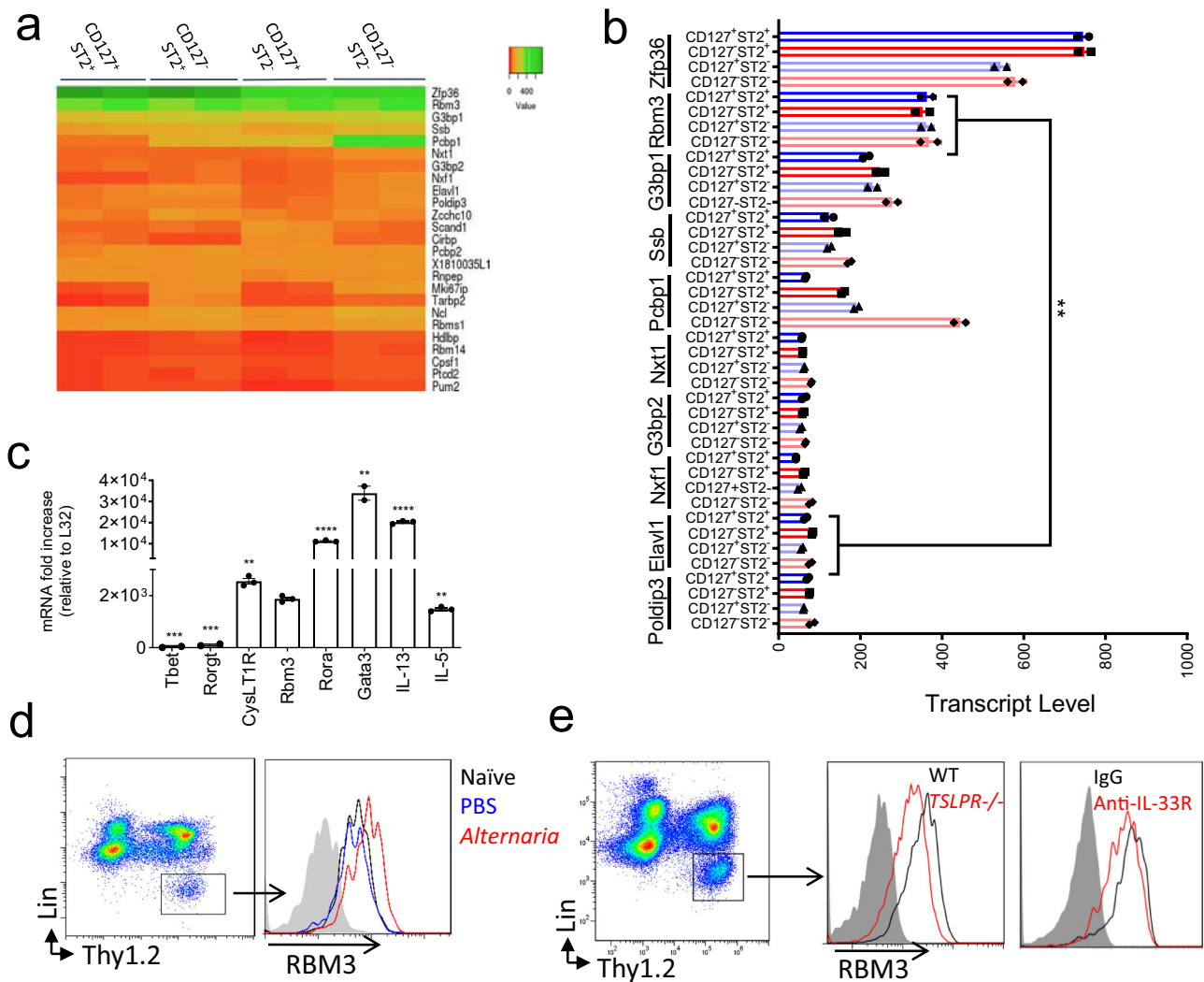


Fig. 1 | RNA-binding protein RBM3 is highly expressed by lung ILCs during fungal allergen exposure and is regulated by IL-33 and TSLP. **a** Wild-type mice were challenged 4 times with 50 μ g *Alternaria* over the span of 10 days and four ILC subsets (CD127⁺ST2⁺, CD127⁺ST2⁻, CD127⁻ST2⁺, CD127⁻ST2⁻) were sorted and collected for RNA-seq. Heatmap showing the relative expression of the top 25 most highly expressed RBPs in the four ILC subtypes. RBPs involved in the cell cycle or splicing were excluded. Statistics were performed with Centroid linkage and Manhattan clustering. **b** Absolute transcript levels of the top 10 RBPs in the four ILC subtypes. Statistics were performed with an unpaired t-test, two-tailed. Data representative of 2 samples ($p < 0.01$). **c** RBM3 mRNA levels of ILC2s in comparison

to several traditional ILC2 mRNA (IL-5, IL-13, Gata-3, Rora, and CysLT1R) and non-ILC2 mRNAs (Rorgt and Tbet). ILC2s were from *Alternaria* challenged mice. Data are from triplicate samples and analyzed with an unpaired t-test, two-tailed. **d** RBM3 expression on ILC2s from naive, PBS challenged, or *Alternaria* challenged lung. Black = Naive, Blue = PBS challenged, Red = *Alternaria* challenged (24 h). **e** RBM3 expression on lung ILC2s of *Tslpr*^{-/-} mice and mice treated with anti-IL-33R antibody. Data representative of at least 4 mice (paired) per group. Mice were challenged with *Alternaria* four times. Grey = isotype control, Black = Wild-Type or IgG treated, Red = *Tslpr*^{-/-} or anti IL33R treated. * $p < 0.05$, ** $p < 0.01$, *** $p < 0.001$. Data are presented as mean values \pm SEM.

sections stained for H&E and PAS displayed increased peribronchial inflammation and mucus production in *Rbm3*^{-/-} mice (Fig. 2f). Thus, *Rbm3*^{-/-} mice exhibited increased type 2 inflammation compared to WT mice in multiple *Alternaria* challenge models.

RBM3 suppresses *Alternaria*-induced lung ILC responses

We next measured ILC activation and proliferation in the lungs of *Rbm3*^{-/-} mice challenged with *Alternaria*. Lung ILCs identified as CD45⁺ lineage-negative Thy1.2⁺ lymphocytes were increased in both number and percent in *Rbm3*^{-/-} mice compared with WT mice (Fig. 3a). Further, lung Ki-67⁺ proliferating ILCs were also increased significantly in *Rbm3*^{-/-} mice (Fig. 3b). ILC2s identified by their production of IL-5 and IL-13 were higher in the *Rbm3*^{-/-} mice compared with WT mice (Fig. 3c). Interestingly, ILCs from *Rbm3*^{-/-} mice demonstrated significantly higher production of IL-17A which may be produced by iILC2s (or ILC2-17s) and/or ILC3s (Fig. 3d)^{2,9,10}. Dual staining of IL-5⁺IL-17⁺ ILCs and IL-

13⁺IL-17a⁺ ILCs showed increases in IL-17 from Th2 cytokine-producing *Rbm3*^{-/-} ILCs compared to WT ILCs, suggesting that these cells may be ILC2₁₇ cells (Fig. 3e, Supplementary Fig. 5f).

The effects of global RBM3 deficiency were not limited to ILCs. After *Alternaria*-challenges, the total number of ST2⁺ CD4⁺ T cells in BAL and lung were greater in *Rbm3*^{-/-} mice compared to WT control (Supplementary Fig. 6a). Ki-67 expression within ST2⁺ T cells was also significantly increased in *Rbm3*^{-/-} mice. ST2 expression within T cells also trended higher in *Rbm3*^{-/-} mice lung and BAL (Supplementary Fig. 6b, c). Thus, it is plausible that RBM3 also directly or indirectly suppresses CD4⁺ Th2 cell responses.

To better assess the function of RBM3 in ILCs independent of T cells, we created double deficient *Rbm3*^{-/-}*Rag2*^{-/-} mice. Consistent with the findings in single knockout *Rbm3*^{-/-} mice, the *Rbm3*^{-/-}*Rag2*^{-/-} mice demonstrated significantly higher lung ILCs, Ki-67-expressing ILCs, and type 2 cytokine-producing ILC2s compared to *Rag2*^{-/-} mice

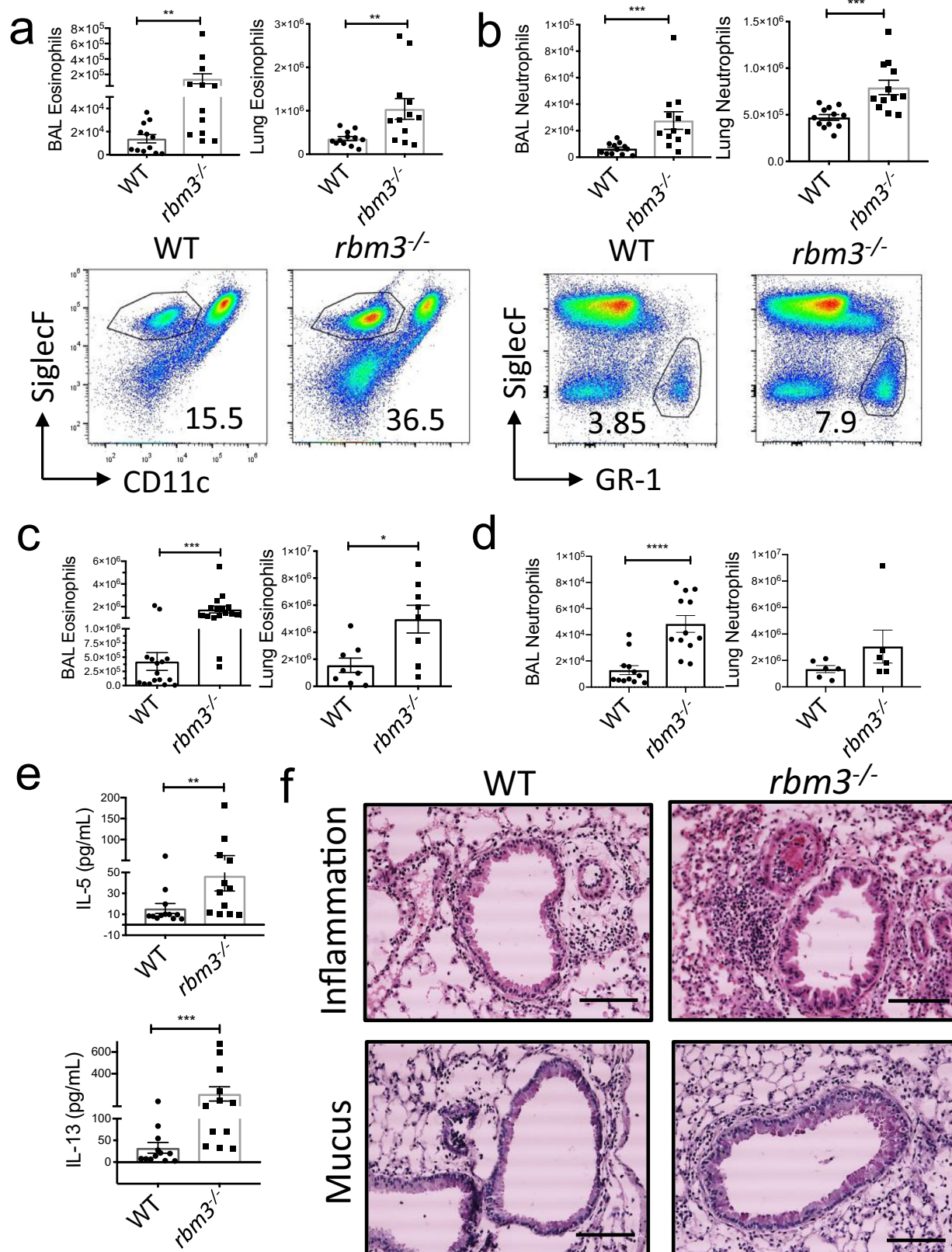


(Fig. 4a–c). BAL and lung eosinophils were also significantly increased in the double knock-out mice compared to controls (Fig. 4d). Overall, these results show a suppressive effect of RBM3 in type 2 lung inflammation and ILC activation, even in the absence of adaptive immunity.

RBM3 directly suppresses IL-33-induced ILC responses in vitro and in vivo

To establish whether RBM3 directly regulated ILC responses, we performed studies with IL-33-stimulated ILCs in vitro and in vivo. FACS sorted WT and *Rbm3*^{-/-} lung Lin⁺Thy1.2⁺ ILCs from *Alternaria*-

Fig. 2 | *Alternaria*-challenged *Rbm3*^{-/-} mice exhibit significant increases in airway granulocytes, inflammation, and Th2 cytokines. Wild-type and *Rbm3*^{-/-} mice were challenged with 10 μ g *Alternaria* three times over 7 days. Data shown are representative of 3 experiments (4 mice per group). **a** Total BAL ($p = 0.0036$) and lung eosinophils ($p = 0.0083$). Representative FACS plots of WT and *Rbm3*^{-/-} mice. Mann-Whitney Test, two-tailed. **b** Total BAL ($p = 0.0001$) and lung ($p = 0.0001$) neutrophils. Representative FACS plots of WT and *Rbm3*^{-/-} mice. Statistics analyzed by Mann-Whitney Test, two-tailed. Wild-type and *Rbm3*^{-/-} mice were challenged

with 20 μ g and 10 μ g *Alternaria* over the span of 10 days. Data shown are representative of 4 experiments (4 mice per group). **c** Total BAL ($p = 0.0001$) and lung ($p = 0.0148$) eosinophils. Mann-Whitney Test, two-tailed. **d** Total BAL ($p < 0.0001$) and lung ($p = 0.2087$) neutrophils. Unpaired *t*-test, two-tailed. **e** BAL levels of Type 2 cytokines (IL-13 $p = 0.0005$ and IL-5 $p = 0.0036$). Mann-Whitney Test, two-tailed. **f** H&E and PAS lung sections at 20X; scale bar is 100 μ m. Airway images representative of 4 mice per group. * $p < 0.05$, ** $p < 0.01$, *** $p < 0.001$, **** $p < 0.0001$. Data are presented as mean values \pm SEM.

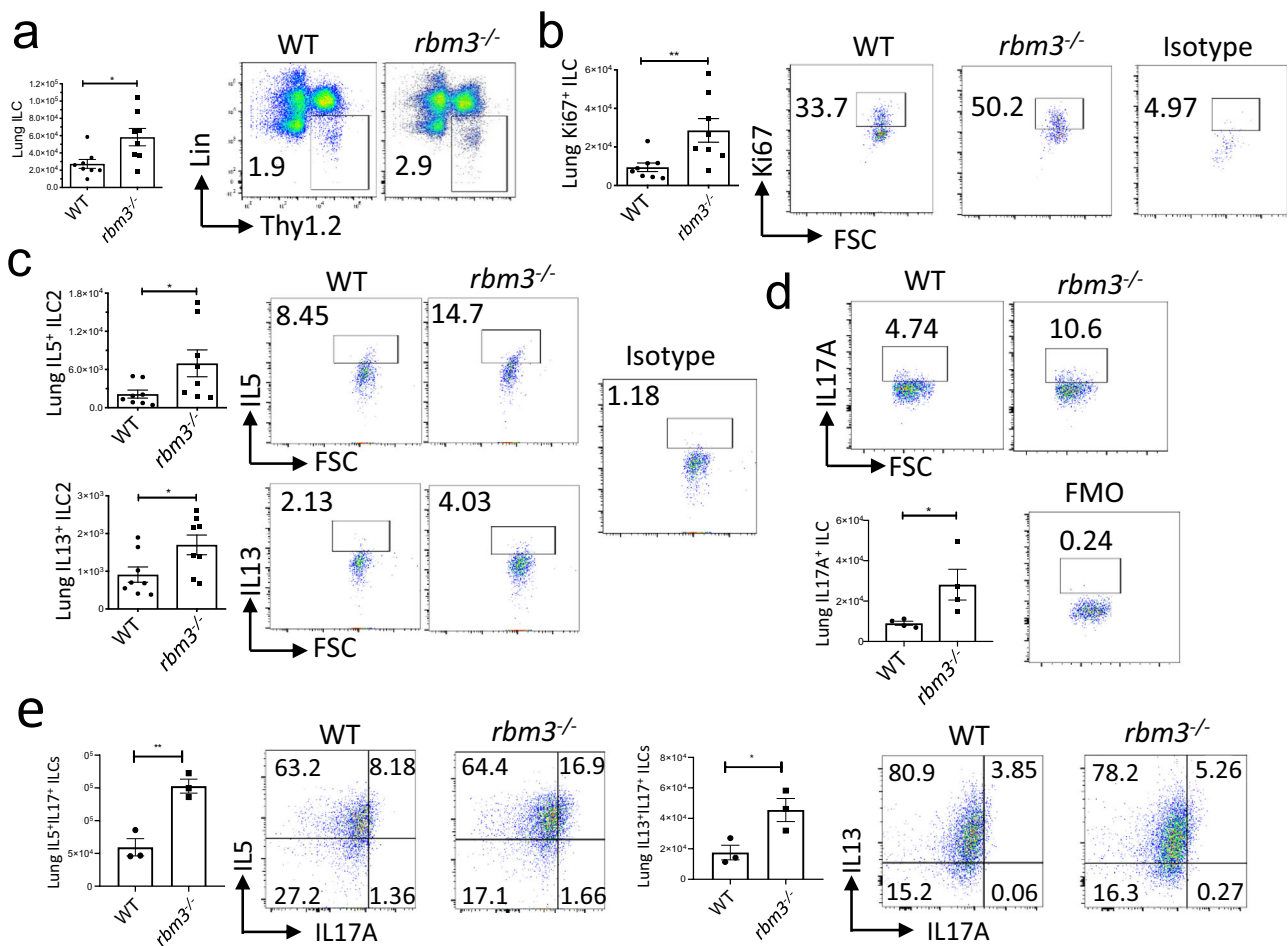


Fig. 3 | ILC2s are increased in *Rbm3*^{-/-} mice and show increased Th2 and IL-17 cytokine production. Wild-type and *Rbm3*^{-/-} mice were challenged with 20 μ g and 10 μ g *Alternaria* over the span of 10 days. Data shown are representative of 4 experiments (4 mice per group). **a** Lung Lin T1ST2⁺ ILC totals ($p = 0.0207$) and FACS plots of LinThy1.2⁺ population. Mann-Whitney Test, two-tailed. **b** Totals of Ki-67 expressing lung ILCs ($p = 0.0070$). FACS plots of Ki-67 percentages and an isotype control. Mann-Whitney Test, two-tailed. **c** Total IL5 ($p = 0.0379$) and IL13 ($p = 0.0379$) expressing lung ILCs. FACS plots of type 2 cytokines percentages and an isotype control. Mann-Whitney Test, two-tailed. Data representative of 4 mice per group. **d** Total IL17A-expressing ILCs ($p = 0.0478$) and representative FACS

plots showing IL17A⁺ ILC percentages. Unpaired *t*-test, two-tailed. Data representative of 4 mice. WT and *Rbm3*^{-/-} mice were challenged intranasally with 25 μ g *Alternaria* 3 times over 7 days. **(e, top)** Total number and percent of ILCs producing IL5 and IL17 in WT and *Rbm3*^{-/-} mice ($p = 0.0053$). FACS plots are representative of one experiment with 3 mice per group. **(e bottom)** Total number and percent of ILCs producing IL13 and IL17 in WT and *Rbm3*^{-/-} mice. ($p = 0.0360$). FACS plots are representative of one experiment with 3 mice per group, isotype controls shown for **b–e**. Unpaired *t*-Test, two-tailed. * $p < 0.05$, ** $p < 0.01$, *** $p < 0.001$. Data are presented as mean values \pm SEM.

challenged mice were rested for 48 h in media alone prior to stimulation. Immediately prior to stimulation, *Rbm3*^{-/-} ILC2s produced significantly more IL-5 by ELISA than wild-type ILC2s (Fig. 5a). In contrast, there were no differences in the production of IL-13 prior to stimulation. IL-33 stimulation (15 ng/ml) of *Rbm3*^{-/-} ILCs resulted in increased IL-5 and IL-13 compared with wild-type ILCs (Fig. 5b). ILCs lacking RBM3 produced significantly more IL-5 after stimulation with IL-33 (both 15 and 30 ng/ml IL-33). Consistent with data in Fig. 3d, ILC IL-17A production was increased in *Rbm3*^{-/-} ILCs after 48 h of rest (Fig. 5c). Unlike the Type 2 cytokines, IL-17A was not

further increased above pre-stimulation conditions with IL-33 stimulation (Fig. 5c). These results demonstrate a direct inhibitory regulatory function of RBM3 in ILC type 2 cytokine production in response to IL-33, as well as a suppressive effect of RBM3 in IL-17A production measured ex vivo.

To assess a direct effect of RBM3 function in ILCs in vivo, *Rbm3*^{-/-} and WT mice were administered IL-33 intranasally which directly activates lung ILC2s^{27,28}. Similar to *Alternaria*-challenged mice, direct challenge with IL-33 led to significantly greater lung Lin⁺Thy1.2⁺ ILCs as well as Ki-67⁺ proliferating ILCs in *Rbm3*^{-/-} mice

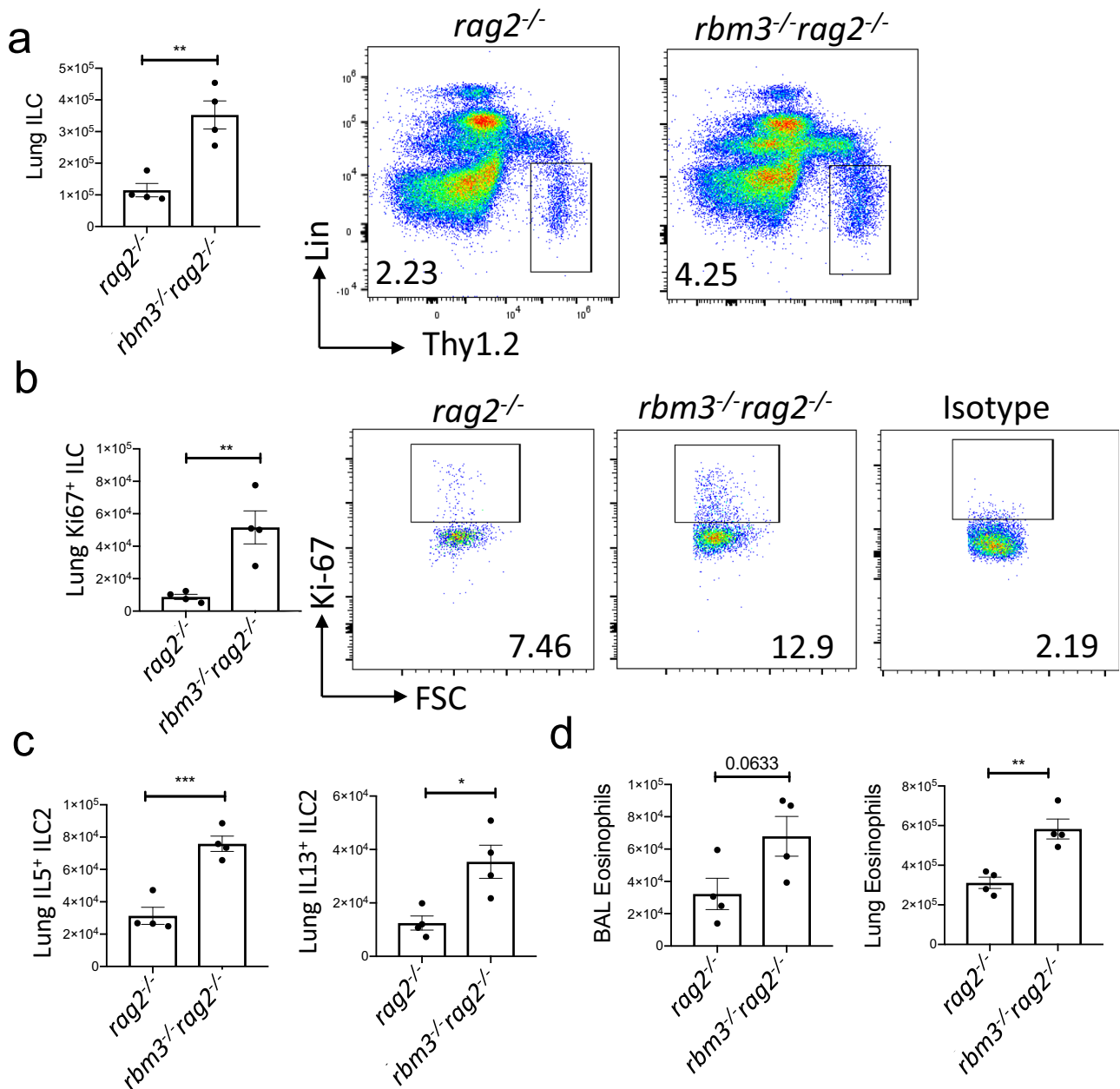


Fig. 4 | RBM3 suppresses lung ILC2s independent of adaptive immunity. $Rag2^{-/-}$ and $Rbm3^{-/-}Rag2^{-/-}$ mice were challenged with 20 μ g *Alternaria* four times over 10 days. Data representative of 4 mice per group. **a–c** Total number of ILCs ($p = 0.0029$), Ki67 expressing ILCs ($p = 0.0060$), and type 2 cytokine-

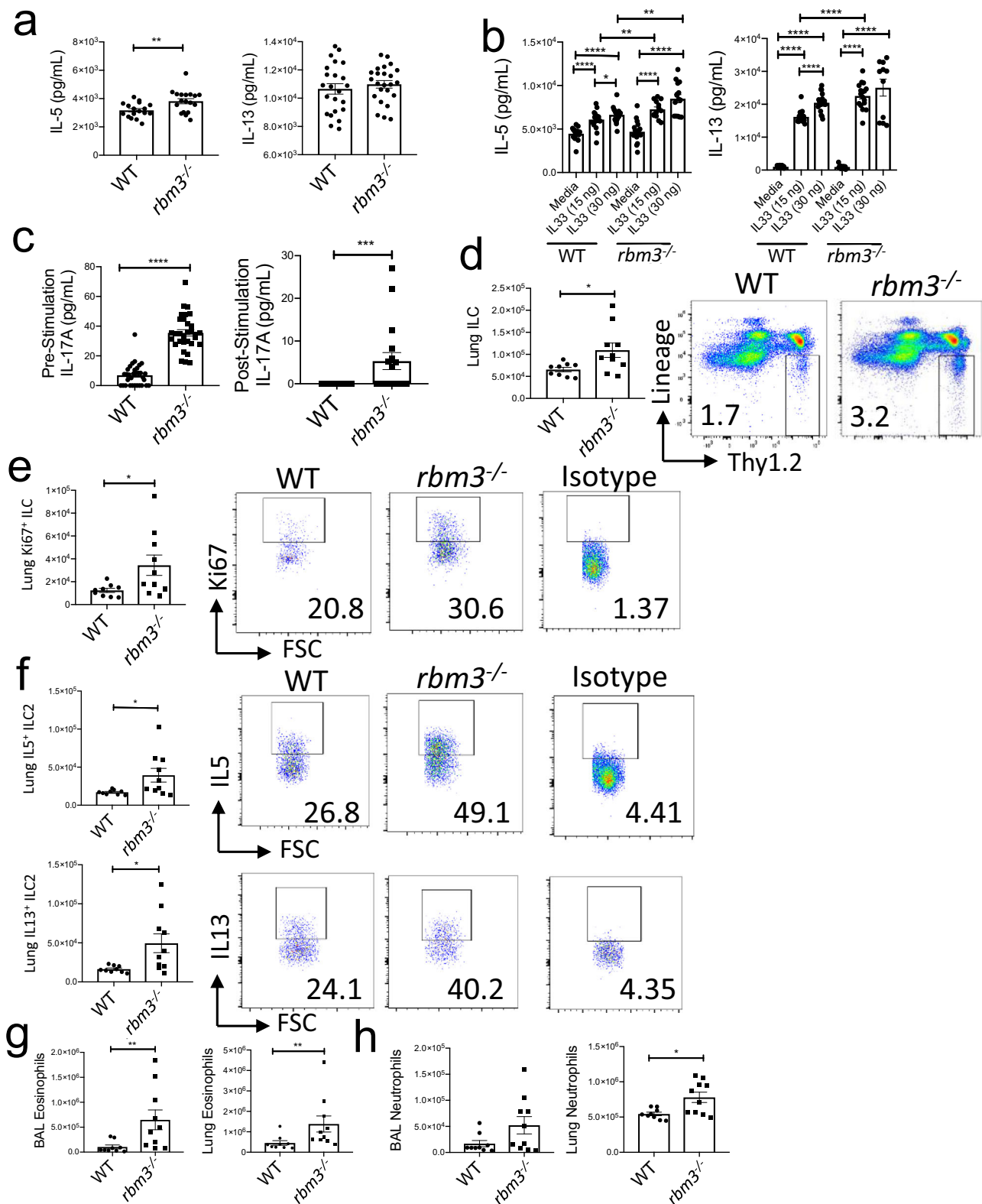
producing ILC2s (IL-5 $p = 0.0008$ and IL-13 $p = 0.0145$). Unpaired *t*-Test, two-tailed. **d** Total BAL ($p = 0.0633$) and lung ($p = 0.0034$) eosinophils. Unpaired *t*-Test, two-tailed. * $p < 0.05$, ** $p < 0.01$, *** $p < 0.001$. Data are presented as mean values \pm SEM.

compared to WT control mice (Fig. 5d, e). Further, $Rbm3^{-/-}$ lung cells had significantly higher IL-5 and IL-13 producing ILC2s (Fig. 5f). BAL and lung eosinophilia were also significantly increased in $Rbm3^{-/-}$ mice (Fig. 5g). Overall, neutrophils in BAL and lung were also increased in $Rbm3^{-/-}$ mice treated with IL-33 (Fig. 5h). Thus, RBM3 directly suppresses lung ILC activation by IL-33 in vitro and in vivo, and this leads to significant differences in eosinophilia and neutrophilia in vivo.

RBM3 intrinsically suppresses lung ILC2 responses

We next generated mixed bone marrow chimera mice by irradiating congenic heterozygote mice ($CD45.1^{+}CD45.2^{+}$) and injecting a 1:1 ratio (10×10^6 cells each) of WT and $Rbm3^{-/-}$ bone marrow cells (Fig. 6a). After 10–12 weeks of reconstitution, mice were challenged with 20 μ g *Alternaria* three times over 7 days. ILC Ki-67

expression and type 2 cytokine production was analyzed from Lin⁺Thy1.2⁺ ILCs from $CD45.1^{+}$ or $CD45.2^{+}$ bone marrow cells (Fig. 6b, Supplementary Fig. 8c). Type 2 cytokine production from $CD45.2^{+}Rbm3^{-/-}$ ILCs was significantly increased compared to WT ILCs, as shown in the percentage and absolute number of IL-5⁺ ILC2s (Fig. 6c, Supplementary Fig. 8c) as well as the percentage and absolute number of IL-13⁺ ILC2s (Fig. 6d, Supplementary Fig. 8c). In addition, Ki-67 expression was significantly increased in $Rbm3^{-/-}$ ILCs compared to WT ILCs (Fig. 6e). In contrast, $Rbm3^{-/-}CD45.2^{+}Lin^{+}Thy1.2^{+}$ cells, which are largely made up of T cells, did not show any change in proliferation or Type 2 cytokine production (Supplementary Figs. 7, 8d) suggesting a more selective intrinsic effect on ILCs. $CD45.2^{+}Rbm3^{-/-}$ lung BAL eosinophils were only slightly increased over $CD45.1^{+}$ WT eosinophils (Supplementary Fig. 8a, b).



Activated ILC programs including increased CysLT1R expression are present in the *Rbm3*^{-/-} ILC transcriptome

We next performed RNA-seq analysis of FACS-sorted Lin⁻Thy1.2⁺ ILCs from WT and *Rbm3*^{-/-} mice (99.4% pure) to more broadly understand the mechanisms by which RBM3 inhibits lung ILC responses (Supplementary Fig. 9). Heat map analysis of common ILC transcripts, particularly those related to ILC2s and ILC3s, were more highly expressed in

Rbm3^{-/-} ILCs than WT controls (Fig. 7a). Principle component analysis showed clear consistent global differences between WT and *Rbm3*^{-/-} ILC transcriptomes (Fig. 7b). Several candidate cytokine transcripts were greater in *Rbm3*^{-/-} ILCs compared with WT ILCs including *Il4*, *Il5*, *Il13*, *Areg*, *Tnf*, *Il17a*, *Il17f*, and *Il22* (Fig. 7c, Supplementary Fig. 10a). The ILC1 cytokine *Ifng* was not significantly different in *Rbm3*^{-/-} ILCs (Supplementary Fig. 10a) and may reflect that RBM3 modulates type 2

Fig. 5 | RBM3 shows a suppressive effect in ILC2s stimulated with IL-33 in vitro and in vivo. WT and *Rbm3*^{-/-} mice were intranasally challenged four times with 50 µg *Alternaria* over 10 days. LinThy1.2⁺ ILC2s were FACS sorted from mouse lung and were rested with 10 ng/mL IL-2 and IL-7 for 48 h prior to stimulation with IL-33. (A) IL-5 ($p = 0.0073$) and IL-13 ($p = 0.4316$) concentration pre-stimulation. Mann-Whitney Test, two-tailed. $n = 17$ – 24 samples from 2 experiments. (B) IL-5 and IL-13 concentration post-stimulation with 15 ng and 30 ng IL-33. Mann-Whitney Test, two-tailed. $n = 13$ – 20 samples from 2 experiments. * $p < 0.05$, ** $p < 0.01$, *** $p < 0.001$, **** $p < 0.0001$ (C) IL-17A concentration levels pre-stimulation ($p < 0.0001$; $n = 31$ – 32 samples) and post-stimulation ($p = 0.0006$; $n = 17$ and 20 samples) with 30 ng IL-33. Mann-Whitney Test, two-tailed. WT and *Rbm3*^{-/-} mice were intranasally

challenged with 10 ng IL-33 three times over 7 days. $n = 9$ – 10 mice per group. (D) Total LinThy1.2⁺ ILCs ($p = 0.0172$) and representative FACS plots. Mann-Whitney Test, two-tailed. (E) Total Ki-67-expressing ILCs ($p = 0.0279$) and representative FACS plots, isotype shown. Mann-Whitney Test, two-tailed. (F) Total number of IL5-expressing ILC2s ($p = 0.0220$) and IL13-expressing ILC2s ($p = 0.0101$) and representative FACS plots of cytokine levels. Cells were cultured for 3 h with cell stimulation cocktail prior to staining, isotypes shown in E&F. Mann-Whitney Test, two-tailed. (G) Total BAL ($p = 0.0041$) and lung ($p = 0.0057$) eosinophils. Mann-Whitney Test, two-tailed. (H) Total BAL ($p = 0.1564$) and lung ($p = 0.0279$) neutrophils. Mann-Whitney Test, two-tailed. * $p < 0.05$, ** $p < 0.01$, *** $p < 0.001$, **** $p < 0.0001$. Data are presented as mean values ± SEM.

cytokine responses and IL-17a production from ILCs or an overall lack of ILC1 responses in the *Alternaria* model. *Rbm3*^{-/-} ILCs also demonstrated increases in relevant ILC surface markers including *Il1r1l*, *Il2rg*, *Cyslt1r*, *Il1rap*, *Cd44*, *Klrg1*, and *Icos* (Supplementary Fig. 10b). Interestingly, while type 2 cytokine transcripts were upregulated in *Rbm3*^{-/-} ILCs, *Gata3* levels were not increased at a transcript or protein level (Supplementary Fig. 10c, g) suggesting other signaling factors are responsible for the increased ILC type 2 cytokine production in *Rbm3*^{-/-} ILCs. Transcription factors known to influence the development, differentiation, or activation of ILCs (including *Tox*²⁹, *Ets1*³⁰, *Rora*^{31,32}, *Irf4*³³, and *Ed2*²) were upregulated in *Rbm3*^{-/-} ILCs, (Supplementary Fig. 10c). Anti-apoptotic and survival transcripts, including *Bcl2*¹, *Cflar*³⁴, *Bcl2a1d*³⁵, and *Hbixip*^{36,37}, were also moderately or significantly upregulated in *Rbm3*^{-/-} ILCs (Supplementary Fig. 10d). BCL2 protein expression was also higher in ILCs from *Alternaria*-challenged *Rbm3*^{-/-} mice than WT controls (Supplementary Fig. 10e) suggesting a potential survival benefit to the *Rbm3*^{-/-} ILCs. Id2 protein expression was also higher in ILC from *Alternaria*-challenged *Rbm3*^{-/-} mice (Supplementary Fig. 10f). *Rbm3*^{-/-} ILCs had increased *Nfact2* expression (encodes NFAT1) which could be a candidate mechanism responsible for increased ILC type 2 cytokine production as NFAT1 mediates ILC2 activation via CysLTR1^{10,38,39} to produce Th2 and Th17 cytokines (Fig. 7c). Though RBM3 binds to the AU-rich regions of mRNAs, there was no correlation between the number of AUUUA (preferentially bound by RBM3) or total ARE regions and the log fold change of differentially expressed transcripts (Supplementary Fig. 11). Therefore, the AU-rich density of transcripts was not predictive of RBM3 regulation of ILC transcriptome differences.

Enhanced lung inflammation and ST2⁺IL-17⁺ ILC accumulation in *Rbm3*^{-/-} mice is dependent on CysLTR1

Given the increased expression of CysLTR1 and NFAT1 in *Rbm3*^{-/-} ILCs, we crossed *Rbm3*^{-/-} mice to *Cyslt1r*^{-/-} mice to generate *Rbm3*^{-/-}*Cyslt1r*^{-/-} double knockout mice that were then challenged with *Alternaria* three times for 14 days. As expected, there was an increase in lung ILC type 2 cytokine and IL-17a production and eosinophilia in *Rbm3*^{-/-} mice compared to WT mice (Fig. 7d). ILC IL-5 and IL-13 production trended toward reduction, but not significantly, in *Rbm3*^{-/-}*Cyslt1r*^{-/-} mice compared to *Rbm3*^{-/-} mice. However, ST2⁺IL-17⁺ ILCs (ILC2-17s) as well as eosinophils were significantly reduced in double knockout mice. Taken together, this suggests that CysLTR1 contributes to RBM3-mediated suppression of lung eosinophilia and ILC2-17 responses.

Discussion

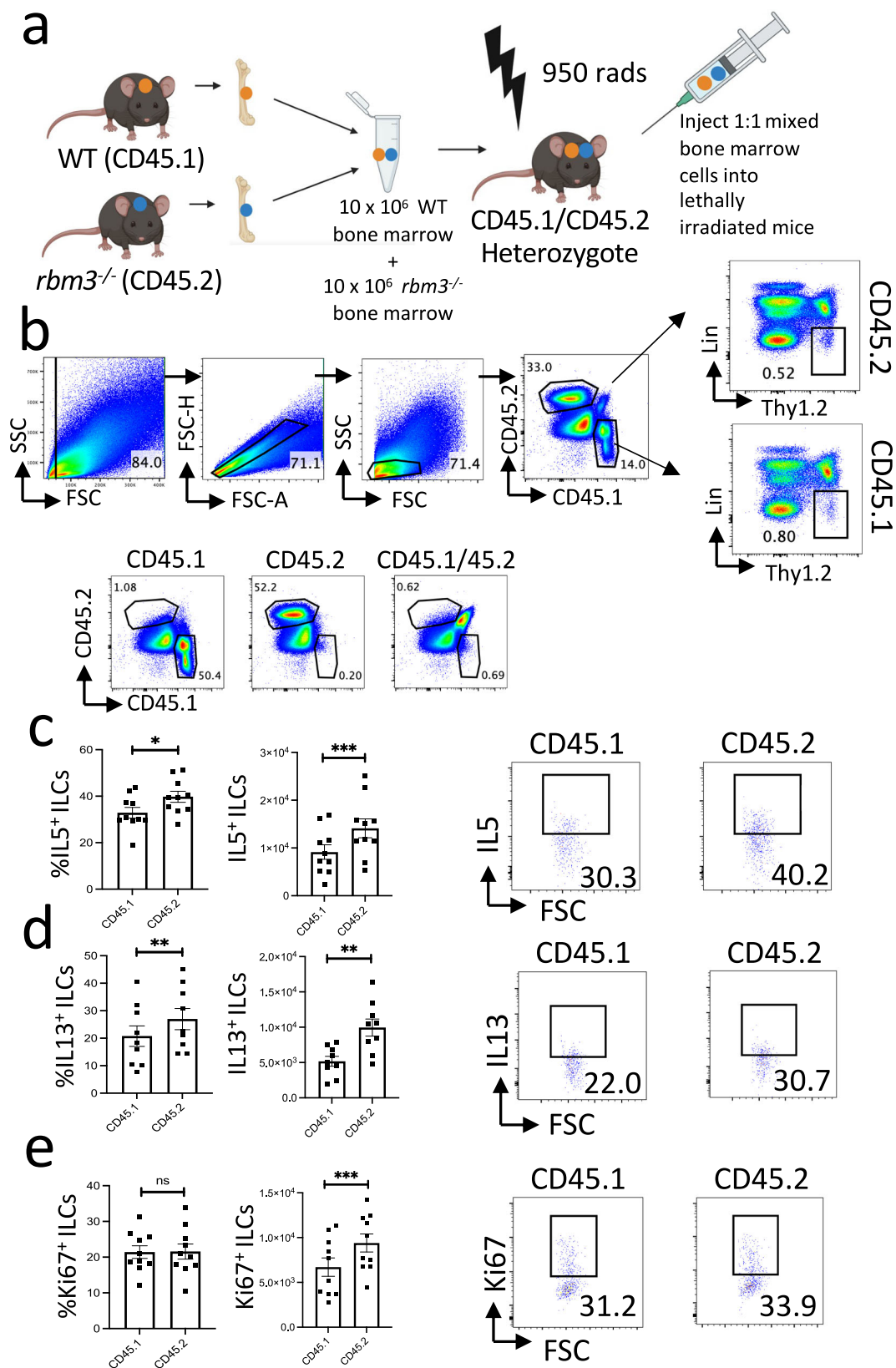
Innate lymphoid cells including ILC2s have recently emerged as critical contributors to immune-mediated diseases including asthma^{40,41}. The majority of the ILC literature thus far has reported soluble factors that activate or inhibit ILC2 function including cytokines and lipid mediators⁴². However, an understanding of intracellular mechanisms that more broadly control ILC function might provide important insights into ILC-driven immune diseases. Studies thus far have demonstrated that specific miRNAs activate ILC2s through multiple mechanisms^{15,16}. Here, we found that RBM3 is a highly expressed RNA-

binding protein (RBP) in lung ILC subsets which is induced by epithelial cytokines IL-33 and TSLP, and negatively regulates ILC type 2 and 17 cytokine production. Mixed bone marrow congenic chimera mice displayed increased type 2 cytokine production in ILCs from *Rbm3*^{-/-} mice, highlighting an ILC-intrinsic activity of RBM3. Further, transcriptomic analysis demonstrated broad differences in *Rbm3*^{-/-} ILCs including expression of CysLTR1, which we found to regulate ILC2 IL-17⁺ cell and eosinophil accumulation in *Rbm3*^{-/-} mice.

RBM3 is a 17KD RNA-binding protein that promotes mRNA stability and translation efficiency by binding to ARE binding regions. Very little is understood about RBM3 in inflammation and immunity. One report showed that RBM3 is downregulated in febrile illness and knockdown of RBM3 led to increases in miRNAs that suppress *PGE2*, *IL6*, and *IFNA1*²³. However, earlier studies showed that RBM3 deficient mice had normal numbers of NK, T, and B cells and had no differences in innate cytokine responses to the TLR9 ligand CpG⁴³. Stressors such as tissue hypoxia and low temperatures can induce RBM3 expression⁴⁴. Our work demonstrates that RBM3 is induced by IL-33 and/or TSLP in mouse and human ILC2s. Of note, IL-33 has been reported to promote a tumor hypoxic microenvironment, with generation of reactive oxygen species, that could lead toward an indirect induction of RBM3 through local hypoxia^{45,46}. Further, in addition to hypoxia and hypothermia, activation of NF-κB promotes RBM3 expression and extracellular IL-33 activates NF-κB^{47,48}. Thus, there may be multiple mechanisms by which IL-33 and/or TSLP may induce RBM3 expression under inflammatory stress conditions.

We found that RBM3 suppresses the classic ILC2 cytokines (IL-5 and IL-13) as well as IL-17A and ILC proliferation. Furthermore, exacerbation of type 2 responses in *Rbm3*^{-/-} mice was independent of changes in total ILC GATA3 levels and lacked correlation with number of ILC AU-rich element (ARE) transcripts. RBM3 has a multitude of complex potential mechanisms that regulate cellular changes during stress including controlling translation efficiency through ARE binding, protein-protein interactions, and effects on miRNAs directly or through dicer processing^{17,23,44}. Interestingly, RBM3 has also been reported to inhibit the p38 MAP kinase pathway which promotes cytokine production by ILC2s in response to IL-33^{49–51}. Thus, removal of RBM3's inhibition of the p38 pathway in ILCs may result in increased cytokine production in *Rbm3*^{-/-} ILCs. Our studies also demonstrate that RBM3 has no effect on ILC2 numbers and lung eosinophilia under homeostatic naïve conditions but has a clear suppressive function during type 2 inflammatory insult. This is consistent with RBM3 being previously identified as a “stress-response” protein that is largely protective in neural survival in conditions of stress⁴⁴. Our data suggest that RBM3 limits hyperactive ILC responses which could be an important protective mechanism during lung inflammation.

In this study, we took a broad approach to ILC identification and included lineage-negative Thy1.2⁺ lymphocytes as ILCs based on our recent work showing that CD127 and ST2 exclude approximately 40% of Th2 cytokine-producing ILC2s²¹. Further, several studies have demonstrated significant heterogeneity and plasticity of ILCs (reviewed in⁵²). For example, in addition to conventional ILC3s, IL-17 production occurs from other ILC sources including “inflammatory”



iILC2s (or ILC2-17s) induced by IL-25, cysteinyl leukotrienes, and Notch signaling^{9,10,53}. Initial reports showed that ST2-negative ILC2s were “inflammatory” ILCs that produce IL-17A in response to IL-25⁹. However, Cai et al. subsequently reported that ST2⁺ ILC2s are also key IL-17A producers (known as ILC2-17s) which can also be induced by CysLTs¹⁰. Similarly, dual cytokine staining in our studies showed that

ILC2s were the dominant ILC source of IL-17 in our models. Despite these results, we cannot exclude the presence of independent populations of ILC3s or other IL-17A-producing ILCs that are regulated by *Rbm3*^{-/-} mice in different contexts.

RBM3 is expressed in multiple immune cells, including eosinophils, macrophages, and T cells. However, we investigated the direct

Fig. 6 | Mixed bone marrow chimeras show cell-intrinsic exaggeration of a type 2 response in ILCs from *Rbm3*^{-/-} mice. **a** Schematic of bone marrow reconstitution. Mixed bone marrow chimeras were generated using bone marrow from CD45.1 *Rbm3*^{+/+} (WT) mice and CD45.2 *Rbm3*^{-/-} mice and reconstituted for 10–12 weeks, images created with BioRender.com. **b** Mixed bone marrow chimera mice were challenged 3 times over 7 days with 20 μg *Alternaria*. FACS plots are representative of 2 independent experiments (5 mice each, *n* = 10) with biological

controls. ILCs are gated as Lineage⁻ Thy1.2⁺ cells. **c** Percent (*p* = 0.0178) and total (*p* = 0.0003) IL5 expressing ILCs from WT vs. *Rbm3*^{-/-} mice. FACS plots of IL5 percentages. **d** Percent (*p* = 0.0012) and total IL13 (*p* = 0.0029) expressing ILCs from WT vs. *Rbm3*^{-/-} mice. Representative FACS plots of IL13 percentages. **e** Percent (*p* = 0.7764) and total Ki67 (*p* = 0.0001) expressing ILCs from WT vs *Rbm3*^{-/-} mice. Representative FACS plots of Ki67 percentages. Paired *t*-Test, two-tailed. **p* < 0.05, ***p* < 0.005, ****p* < 0.0005.

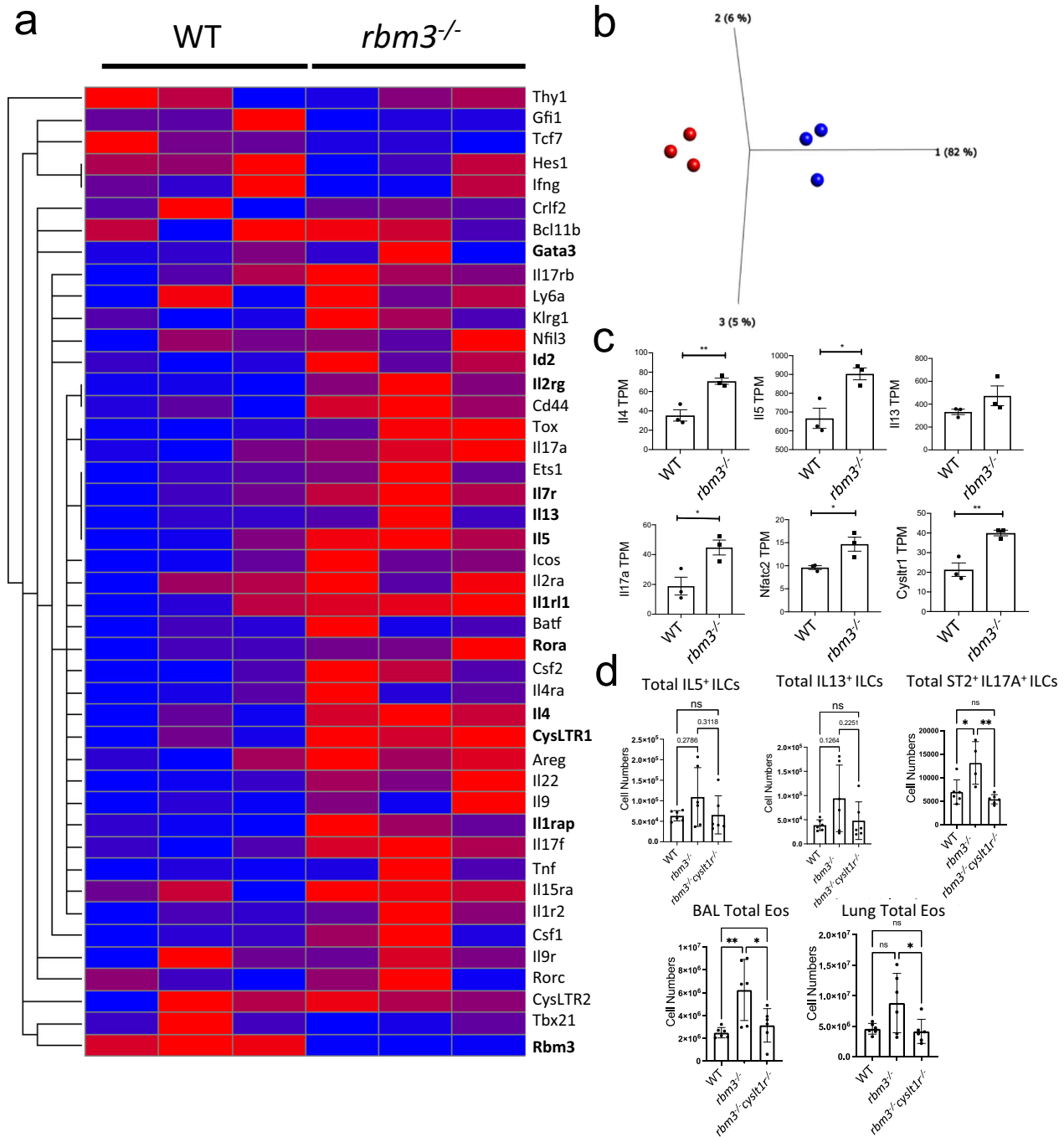


Fig. 7 | CysLT1R controls eosinophilia and ST2⁺IL-17⁺ ILC2 accumulation in *Rbm3*^{-/-} mice. WT and *Rbm3*^{-/-} mice were challenged with 25 μg *Alternaria* three times over 7 days. Lin⁺Thy1.2⁺ ILCs were FACS-sorted and bulk RNA-sequenced. Data representative of three mice per group. **a** Relative transcript levels of select ILC transcripts **b** PCA plot of WT (blue) and *Rbm3*^{-/-} (red) samples. **c** TPMs of select surface marker, cytokine, and transcription factor transcripts. Unpaired *t*-test,

two-tailed. **p* < 0.05, ***p* < 0.01, ****p* < 0.001. **d** Wild-type, *Rbm3*^{-/-}, and *Rbm3*^{-/-} *Cyslr1*^{-/-} mice were challenged with *Alternaria* three times over 14 days. Total type 2 cytokine-producing ILC2s, IL17 producing ST2⁺ILCs, and BAL and lung eosinophils in WT, *Rbm3*^{-/-}, and *Rbm3*^{-/-} *Cyslr1*^{-/-} mice, One way ANOVA. **p* < 0.05, ***p* < 0.01, ****p* < 0.001. Data are presented as mean values ± SEM.

function of RBM3 in lung ILCs given the emerging functions of ILCs during lung inflammation. In the mixed bone marrow chimera studies, we show that Lin⁺Thy1.2⁺ *Rbm3*^{-/-} ILCs were more activated compared with congenic WT ILCs. In contrast, Lin⁺Thy1.2⁺ populations, which largely include T cells, did not demonstrate a significant change in proliferation of type 2 cytokine production between WT and *Rbm3*^{-/-} cells. Thus, it appears that there may be a more selective intrinsic contribution of RBM3 in ILCs during type 2 inflammation compared with T cells. However, Th2 cells were increased in the complete *Rbm3*^{-/-} mice after *Alternaria* challenges and this may be due to early ILC2 contributions to adaptive Th2 responses as previously reported^{54,55}.

To explore potential mechanisms by which RBM3 regulates ILC biology, we performed transcriptomic studies which demonstrated global changes in activation of ILCs by RBM3 including differential expression of known ILC cytokines, receptors as well as transcription factor, and survival transcripts. Importantly, cytokine transcript data from *Rbm3*^{-/-} ILCs supported our *in vivo* findings that RBM3 suppressed type 2 and IL-17A cytokine production from ILCs. Transcripts for multiple receptors were increased in *Rbm3*^{-/-} ILCs, including *Il1r1* (encodes ST2), *Il7r*, *Il2rg*, *Cysltr1*, and *Cd44*. Though *Il1r1* was increased at a transcript level, we did not detect increased ST2 at a protein level by flow cytometry. Notably, several ILC transcription factors were increased in *Rbm3*^{-/-} ILCs including *Tox*, *Ets1*, *Rora*, *Irf4*, and *Id2*^{29–33}. ROR α and ETS1 also promote ILC2 cytokine production suggesting ILC2 cytokine production could be regulated by RBM3 through control of these transcription factors^{30,56}. Despite differences in levels of developmental transcription factors in *Rbm3*^{-/-} ILCs, we did not detect differences in lung ILCs in naive *Rbm3*^{-/-} mice. This may be explained by induction of RBM3 in inflammatory settings which exerts effects on mature ILCs while being dispensable for ILC development.

Increased expression of the *Cysltr1* transcript in *Rbm3*^{-/-} ILCs was a particularly interesting finding because it was accompanied by an increase in expression of *Nfat2c* (encodes NFAT1). Previous reports have shown that CysLT1R signaling in ILCs is regulated by NFAT1 to promote increased Th2 and Th17 cytokine production^{10,38,57,58}. Therefore, we generated *Rbm3*^{-/-}*Cysltr1*^{-/-} double knockout mice, which showed that CysLT1R regulates some of the hyperinflammatory phenotype observed in *Rbm3*^{-/-} mice after *Alternaria* challenges. Interestingly, ST2⁺IL-17⁺ ILCs were also controlled by CysLT1R in *Rbm3*^{-/-} mice which is in line with previous data that CysLTs induce IL-17 from ST2⁺ ILCs¹⁰. As ILC2 responses through CysLT1R are regulated by NFAT1, RBM3 suppression of the CysLT1R/NFAT1 axis could potentially limit ILC-driven lung inflammation though it is likely that other RBM3-dependent mechanisms contribute as well.

In summary, this work identifies an important function of RBM3, a highly expressed RNA-binding protein, in activated lung ILCs that is induced by IL-33 and TSLP. RBM3 dampens both type 2 cytokine and IL-17A cytokine production by lung ILCs and decreases downstream granulocyte infiltration in the setting of fungal allergen and IL-33 exposure. Mixed bone marrow chimera studies highlighted the cell-intrinsic effect of RBM3 on ILC function and transcriptomic analysis demonstrated RBM3 regulation of multiple cytokines, transcription factors, survival genes, and receptors critical to ILC function including CysLT1R. Studies of allergen-challenged *Rbm3*^{-/-}*Cysltr1*^{-/-} double knockout mice demonstrated that CysLT1R contributes to RBM3-mediated ILC responses. The work presented herein further substantiates RNA-binding proteins as critical post-transcriptional regulatory mediators of ILC activation during type 2 inflammation.

Methods

The research complies with all relevant ethical regulations and was approved by the UC San Diego IACUC animal care committee. Reagents for flow cytometry, qPCR, ELISA, allergen, and cytokines detailed in the Supplementary Data file.

Mice

6–12-week-old female and male C57BL/6J mice were obtained from Jackson Laboratories (Bar Harbor, ME). Wild-type mice were age and gender matched to *Rbm3*^{-/-} mice acquired from Peter Vanderklish at TSRI and originally from Tadatsugu Taniguchi⁴³ at University of Tokyo and bred in house. *Tslpr*^{-/-} mice were acquired from Dr. Michael Croft at the La Jolla Institute for Immunology and originally from Dr. Steven Ziegler⁵⁹. The *Rbm3*^{-/-}*Rag2*^{-/-} mice were created through multiple crosses of *Rbm3*^{-/-} and *Rag2*^{-/-} mice and bred in house. The *Rbm3*^{-/-}*Cysltr1*^{-/-} mice were created through seven crosses of *Rbm3*^{-/-} and *Cysltr1*^{-/-} mice (Jax stock number #030814) and bred in house. Mixed bone marrow chimera studies utilized CD45.1⁺ PEP boy homozygotes and CD45.1⁺CD45.2⁺ PEP boy heterozygotes (Jax stock number: #002014). WT and *Rag2*^{-/-} (Jax stock number #008449) mice originated from Jackson labs (Bar Harbor, ME). All mice were on a C57BL/6 background and controls were age and gender matched. All studies were approved by the University of California, San Diego Institutional Animal Care and Use Committee.

Lung inflammation models

Mice were intranasally challenged with *Alternaria alternata* extract (Greer, Lenoir, NC) or recombinant IL-33 (R&D Systems, Minneapolis, MN) diluted in PBS. For the isolation of the ILC subsets for RNA-seq analysis and the isolation of Lin⁺Thy1.2⁺ ILCs for *in vitro* assays, mice were challenged with 50 μ g *Alternaria* 4 times over 10 days. Mice were challenged with 25 μ g *Alternaria* 3 times over 7 days to expand the Lin⁺Thy1.2⁺ ILC population for RNA-seq analysis. Experiments with *Tslpr*^{-/-} mice or the anti-IL-33R blocking antibody involved 4 challenges with *Alternaria*. Various *Alternaria* challenged models were utilized with the *Rbm3*^{-/-} mice. Mice were intranasally challenged three times over 7 days with 10 μ g or 25 μ g *Alternaria* or were challenged once with 20 μ g *Alternaria* followed by 3 challenges of 10 μ g *Alternaria* over 10 days where indicated. WT and *Rbm3*^{-/-} mice were also intranasally challenged with 10 ng recombinant IL-33 3 times over 7 days. *Rag2*^{-/-} and *Rbm3*^{-/-}*Rag2*^{-/-} mice were challenged with 20 μ g *Alternaria* 4 times over 10 days. Wild-type mice were treated with anti-IL-33 antibody (DJ8)²⁶ or control IgG intraperitoneally on Days -1, 0, 3, and 6. For mixed bone marrow chimera studies, mice were challenged 3 times over 7 days with 20 μ g *Alternaria*. WT, *Rbm3*^{-/-}, and *Rbm3*^{-/-}*Cysltr1*^{-/-} mice were challenged with 30 μ g *Alternaria* on D0 and 3 μ g *Alternaria* on D9 and D12 before being sacrificed on D14.

Generation of mixed bone marrow chimeras

Bone marrow was isolated from femurs of donor CD45.2⁺ *Rbm3*^{-/-} mice and CD45.1⁺ WT congenic mice. Recipient CD45.1/CD45.2⁺ mice were lethally irradiated with 950 rads from a cesium irradiator. Irradiated mice were then injected retro-orbitally with a 1:1 ratio of 10 \times 10⁶ CD45.1⁺ and 10 \times 10⁶ CD45.2⁺ bone marrow cells. Mice were analyzed 8 weeks after injection by flow cytometry (single congenic CD45.1 and CD45.2 populations) to confirm successful bone marrow reconstitution.

BAL and lung processing

Bronchoalveolar lavage (BAL) was collected in 2% BSA (Sigma, St. Louis, MO) and supernatant for the first flush of BAL was saved and stored in -20C for ELISA²⁶. Lungs were collected in RPMI and was dissociated into a single-cell suspension using the Miltenyi Lung Digest Kit and Dissociator (Miltenyi Biotec, Bergisch Gladbach, Germany) per the company's protocol. Cells counts were obtained using flow cytometry (Novocyte).

Histology

The left half of the lung was used for histology. Lungs were perfused and fixed in 4% paraformaldehyde. Hematoxylin and Eosin (H&E) and Periodic acid-Schiff (PAS) staining was performed at the Histology Core in UCSD's Moore's Cancer Center and imaged with microscopy as

previously reported²¹. Hematoxylin and Eosin (H&E) and Periodic acid–Schiff (PAS) staining were performed at the Histology Core in UCSD's Moore's Cancer Center and imaged with microscopy as previously reported²¹. H&E and PAS stained slide images were captured at 20X magnification for levels of peribronchial inflammation and PAS stained slides, respectively.

ELISA

Samples stored at –20°C were analyzed using IL-5 and IL-13 ELISA kits (R&D Systems, Minneapolis, MN) per the company's instructions. Plates were read using a microplate reader model 680 (Bio-Rad Laboratories, Hercules, CA). ELISA data was analyzed using Excel and Graphpad Prism (San Diego, CA).

ILC purification and RNA Sequencing

WT and *Rbm3*^{–/–} ILCs or WT ILCs based on ST2 and CD127 expression were sorted with the BD FACSAria II or the BD FACSAria Fusion at the UCSD Human Embryonic Stem Cell Core Facility. Lin[–]Thy1.2⁺ ILCs were sorted directly into TrizolLS. RNA-sequencing was performed at the La Jolla Institute. RNA-sequencing data of *Rbm3*^{–/–} and WT ILCs was newly generated for this study and deposited in GEO database (GSE155330). RNA-sequencing of ILCs based ST2 and CD127 were previously reported²¹ and is deposited in GEO database (GSE136156).

Briefly, purified total RNA (≈5 ng) was amplified following the Smart-seq2 protocol^{60,61}. mRNA was captured using poly-dT oligos and directly reverse-transcribed into full-length cDNA using the described template-switching oligo^{60,61}. cDNA was amplified by PCR for 15 cycles and purified using AMPure XP magnetic bead (0.9:1 (vol:vol) ratio, Beckman Coulter). From this step, for each sample, 1 ng of cDNA was used to prepare a standard NextEra XT sequencing library (NextEra XT DNA library prep kit and index kits; Illumina). Barcoded Illumina sequencing libraries (NextEra; Illumina) were generated utilizing an automated platform (Biomek FXP, Beckman Coulter). Both whole-transcriptome amplification and sequencing library preparations were performed in a 96-well format to reduce assay-to-assay variability. Quality control steps were included to determine total RNA quality and quantity, the optimal number of PCR preamplification cycles, and fragment library size. The reference genome was mm10 (mouse genome). None of the samples failed quality controls. All of the samples were pooled at equimolar concentration, loaded, and sequenced on the Illumina Sequencing platform, HiSeq2500 (Illumina). Libraries were sequenced to obtain more than 10 million 50-bp single-end reads (HiSeq Rapid Run Cluster and SBS Kit V2; Illumina) mapping uniquely to mRNA reference.

qPCR

RNA was reverse transcribed to cDNA using a Transcriptor First Strand cDNA Synthesis Kit (Roche) according to the manufacturer's instructions. RT-PCR was performed using SYBR Green I Master (Roche) and RT-PCR-specific primers. The primer sequences (5'–3') were as follows: *mIL-5* forward AAGAGAAGTGTGGCGAGGAGA; *mIL-5* reverse CACCAAGGAACCTTTCAGGTAA; *mIL-13* forward GAGCAACATCACACAAGACCAGA; *mIL-13* reverse GCCAGTCCACATCCATA; *Cystlr* forward AACGAATATCCACCTTACC; *Cystlr* reverse AGCCTTCCTAAAGTTTCCAC; *L32* forward GAAACTGGCGAAACCCA; and *L32* reverse GGATCTGGCCCTTGAACCTT. qPCR was completed using the *Rbm3* transcript variant 2 (NM_001166409). Transcripts were measured relative to *L32* using Roche LightCycler 480 (Roche Diagnostics)⁵⁸. qPCR performed on CD127^{hi} ST2^{hi} Lin[–]Thy1.2⁺ lymphocytes utilized the following transcripts: *Rbm3* (Mm00812518_m1), *Tsfp* (Mm00497362_m1), *Cystlr1* (Mm02620326_s1), *Il13* (Mm00434204_m1), *Il17a* (Mm00439618_m1), *Cd127* (Mm01309416_m1), and *Thy1.2* (Mm00493681_m1). Transcripts were measured relative to *Hprt* using QuantStudio3 (Thermo Fisher Scientific).

Flow Cytometry

For surface stains, 1 × 10⁶ lung and BAL cells were stained. For intracellular stains, 2 × 10⁶ lung cells were stained. Fc receptors were first blocked for 5 min using CD16/CD32 (Biolegend, San Diego, CA). Eosinophils were identified as CD11c[–]Siglec-F⁺ and neutrophils were identified as Siglec-F[–]GR-1⁺; they were stained using CD45.2 (PerCP), Siglec-F (PE), GR-1(APC), and CD11c (FITC). ILCs were identified as Lineage[–]Thy1.2⁺ lymphocytes or Lineage[–]T1ST2⁺ lymphocytes and were stained using CD45.2 (PerCP), Thy1.2 (APC), T1ST2 (PE), and a lineage cocktail. The lineage cocktail (FITC) consisted of the BioLegend Lineage cocktail (consists of CD3e, Ly-6G/Ly-6C, CD11b, CD45R/B220, and TER-119), CD11c, NK1.1, CD5, FcεR1, TCRαβ, and TCRγδ. The ILC subsets were stained with ST2 (APC) and CD127 (PE-Cy7). For nuclear intracellular staining, cells were permeabilized using the FoxP3 kit (ThermoFisher, Waltham, MA) after surface staining. Cells were stained with Ki-67 (PE or APC), RBM3, GATA3 (PE), and ID2 (PE).

For cytokine intracellular staining of lung cells in the 10-day challenge model, cells were cultured overnight with Golgi Plug (Fisher Scientific, Hampton, NH) at 500,000 cells per well. After surface staining for ILCs, cells were fixed and permeabilized using the BD fixation/permeabilization kit (BD Biosciences, La Jolla, CA) and stained for IL-5 (PE) or IL-13 (PE). For cytokine intracellular staining following the 7-day IL-33 and *Alternaria* challenge model, lung cells were cultured for 3 h with cell stimulation cocktail (ThermoFisher, Waltham, MA) at 1 × 10⁶ cells per well. After surface staining for ILCs, cells were fixed and permeabilized using the BD kit and stained for IL-5 (PE), IL-13 (PE), or IL17A (eFlour506). Lung cells stained for Bcl-2 expression were surface stained for ILCs, fixed and permeabilized with the BD kit, and stained with anti-Bcl-2 (PE-Cy7).

For human PBMC staining, ILC2s were sorted as Lineage[–]CRTH2⁺ lymphocytes. The lineage cocktail (FITC) consisted of antibodies for CD3, CD14, CD16, CD19, CD20, CD56, TCRγδ, CD4, CD11b, CD235a, and FcεR1. The polyclonal RBM3 antibody used in this study was raised in rabbits to the 14 c-terminal amino acids of RBM3, and affinity purified to the immunizing peptide. As described in prior work^{62,63}, the affinity-purified anti-RBM3 antibody recognizes an ~17 kDa band corresponding to RBM3 on Western blots and selectively labels RBM3 in situ under a variety of fixation conditions. Flow Cytometry was performed using the BD Accuri for Fig. 1 and Supplementary Fig. 3b, otherwise, Acea Novocyte was used. Data was analyzed using FlowJo software (Tree Star, Ashland, OR). All antibodies were from Biolegend, ThermoFisher, or BD Biosciences.

Immunofluorescence

For mouse airways, immunofluorescence for RBM3 was performed on naïve and *Alternaria* challenged airways as previously reported^{64,65}. Briefly, lung samples were de-paraffinized by sequential placement in xylene and ethanol. Staining for RBM3 was performed with rabbit polyclonal antibody (PeproTech) at 1:1000 concentration. Tyramide Signal Amplification Kit #41 (Invitrogen) was used for fluorescent signal amplification with subsequent DAPI staining (Vector Laboratories). Lung airways were visualized with a DM2500 microscope (Leica Microsystems). Cell nuclei were stained with DAPI. Images were taken from at least 5 airways of at least 3 mice per group.

ILC and PBMC cultures

WT and *Rbm3*^{–/–} Lin[–]Thy1.2⁺ ILCs were sorted using the BD FACSAria Fusion and BD FACSAria II sorters from UCSD's Human Embryonic Stem Cell Core Facility. Collected ILCs were rested in 10 ng/mL IL-2 and IL-7 (R&D Systems, Minneapolis, MN) in T cell media (RPMI + 10% FBS, 1% glutamine, 0.1% BME, 1% pen/strep) for 48 h. ILCs were cultured in a 96-well plate at 40,000 cells per well. Pre-stimulation media was collected and stored in –80°C for ELISA. ILCs were stimulated for 24 h with 15 ng/mL or 30 ng/mL IL-33 (R&D Systems, Minneapolis, MN) in T cell

media. Post-stimulation supernatant was collected and stored at -80°C for ELISA analysis.

Human PBMCs were isolated from commercially purchased leukopacks (Allcells, Alameda, CA, USA). Human peripheral blood ILC2s were sorted as $\text{CD45}^{\text{lin}}\text{CRTH2}^{\text{+}}$ lymphocytes and cultured and treated with TSLP and IL-33 before being fixed with 4% PFA and processed for immunocytochemistry using a RBM3 antibody (1:2000) and a Cy3 secondary. Cells were also stained for DAPI. Images were taken at 20X. Immuno-positive elements were captured and analyzed by thresholding the intensity histogram in the Cy3 channel at 100. Data for objects of 50–175 pixels were included.

Statistical analysis

Statistical analysis was performed with GraphPad Prism software (GraphPad Software, La Jolla, CA). P-values were obtained using the Mann-Whitney test, unpaired t-test, or one-way ANOVA and a P value of less than 0.05 was considered statistically significant such that $*p < 0.05$, $**p < 0.01$, $***p < 0.001$.

Reporting summary

Further information on research design is available in the Nature Research Reporting Summary linked to this article.

Data availability

Reagents for flow cytometry, qPCR, ELISA, allergen, and cytokines are detailed in the Supplementary Data file. RNA-sequencing data of *Rbm3*^{-/-} and WT ILCs was newly generated and deposited in GEO database ([GSE155330](https://www.ncbi.nlm.nih.gov/geo/query/acc.cgi?acc=GSE155330)). RNA-sequencing of ILCs based ST2 and CD127 was previously reported²¹ and is deposited in GEO database ([GSE136156](https://www.ncbi.nlm.nih.gov/geo/query/acc.cgi?acc=GSE136156)). There are no restrictions with obtaining unique biological materials which are available from the corresponding author upon reasonable request. Source data are provided with this paper.

References

- Moro, K. et al. Innate production of TH2 cytokines by adipose tissue-associated c-Kit+Sca-1+ lymphoid cells. *Nature* **463**, 540–544 (2010).
- Kim, H. Y. et al. Interleukin-17-producing innate lymphoid cells and the NLRP3 inflammasome facilitate obesity-associated airway hyperreactivity. *Nat. Med.* **20**, 54–61 (2014).
- Chang, Y. J. et al. Innate lymphoid cells mediate influenza-induced airway hyper-reactivity independently of adaptive immunity. *Nat. Immunol.* **12**, 631–638 (2011).
- Hams, E. et al. IL-25 and type 2 innate lymphoid cells induce pulmonary fibrosis. *Proc. Natl Acad. Sci. USA* **111**, 367–372 (2014).
- Artis, D. & Spits, H. The biology of innate lymphoid cells. *Nature* **517**, 293–301 (2015).
- Hurrell, B. P., Shafiei Jahani, P. & Akbari, O. Social Networking of group two innate lymphoid cells in allergy and asthma. *Front Immunol.* **9**, 2694 (2018).
- Lambrecht, B. N., Hammad, H. & Fahy, J. V. The cytokines of asthma. *Immunity* **50**, 975–991 (2019).
- Gour, N. & Wills-Karp, M. IL-4 and IL-13 signaling in allergic airway disease. *Cytokine* **75**, 68–78 (2015).
- Huang, Y. et al. IL-25-responsive, lineage-negative KLRG1(hi) cells are multipotential ‘inflammatory’ type 2 innate lymphoid cells. *Nat. Immunol.* **16**, 161–169 (2015).
- Cai, T. et al. IL-17-producing ST2(+) group 2 innate lymphoid cells play a pathogenic role in lung inflammation. *J. Allergy Clin. Immunol.* **143**, 229–244 e229 (2019).
- Moro, K. et al. Interferon and IL-27 antagonize the function of group 2 innate lymphoid cells and type 2 innate immune responses. *Nat. Immunol.* **17**, 76–86 (2016).
- Duerr, C. U. et al. Type I interferon restricts type 2 immunopathology through the regulation of group 2 innate lymphoid cells. *Nat. Immunol.* **17**, 65–75 (2016).
- Maric, J. et al. Prostaglandin E2 suppresses human group 2 innate lymphoid cell function. *J. Allergy Clin. Immunol.* **141**, 1761–1773 e1766 (2018).
- Zhou, W. et al. Prostaglandin I2 signaling and inhibition of Group 2 innate lymphoid cell responses. *Am. J. Respir. Crit. Care Med.* **193**, 31–42 (2016).
- Knolle, M. D. et al. MicroRNA-155 protects Group 2 innate lymphoid cells from apoptosis to promote Type-2 immunity. *Front. Immunol.* **9**, 2232 (2018).
- Singh, P. B. et al. MicroRNA regulation of type 2 innate lymphoid cell homeostasis and function in allergic inflammation. *J. Exp. Med.* **214**, 3627–3643 (2017).
- Pilotte, J., Dupont-Versteegden, E. E. & Vanderklis, P. W. Widespread regulation of miRNA biogenesis at the Dicer step by the cold-inducible RNA-binding protein, RBM3. *PLoS One* **6**, e28446 (2011).
- Stellato, C. et al. Coordinate regulation of GATA-3 and Th2 cytokine gene expression by the RNA-binding protein HuR. *J. Immunol.* **187**, 441–449 (2011).
- Gruber, A. R., Fallmann, J., Kratochvill, F., Kovarik, P. & Hofacker, I. L. AREsite: a database for the comprehensive investigation of AU-rich elements. *Nucleic Acids Res.* **39**, D66–D69 (2011).
- Hikichi, Y., Motomura, Y., Takeuchi, O. & Moro, K. Posttranscriptional regulation of ILC2 homeostatic function via tristetraproline. *J. Exp. Med.* **218**, 1–12 (2021).
- Cavagnero, K. J. et al. Unconventional ST2- and CD127-negative lung ILC2 populations are induced by the fungal allergen *Alternaria alternata*. *J. Allergy Clin. Immunol.* **144**, 1432–1435 e1439 (2019).
- Sureban, S. M. et al. Translation regulatory factor RBM3 is a proto-oncogene that prevents mitotic catastrophe. *Oncogene* **27**, 4544–4556 (2008).
- Wong, J. J. et al. RBM3 regulates temperature sensitive miR-142-5p and miR-143 (thermomiRs), which target immune genes and control fever. *Nucleic Acids Res.* **44**, 2888–2897 (2016).
- Taylor, G. A. et al. A pathogenetic role for TNF α in the syndrome of cachexia, arthritis, and autoimmunity resulting from Tristetraproline (TTP) Deficiency. *Immunity* **4**, 445–454 (1996).
- Casolaro, V. et al. Posttranscriptional regulation of IL-13 in T cells: role of the RNA-binding protein HuR. *J. Allergy Clin. Immunol.* **121**, 853–859 e854 (2008).
- Doherty, T. A. et al. STAT6 regulates natural helper cell proliferation during lung inflammation initiated by *Alternaria*. *Am. J. Physiol. Lung Cell Mol. Physiol.* **303**, L577–L588 (2012).
- Bartemes, K. R. et al. IL-33-responsive lineage- CD25+ CD44(hi) lymphoid cells mediate innate type 2 immunity and allergic inflammation in the lungs. *J. Immunol.* **188**, 1503–1513 (2012).
- Barlow, J. L. et al. IL-33 is more potent than IL-25 in provoking IL-13-producing nuocytes (type 2 innate lymphoid cells) and airway contraction. *J. Allergy Clin. Immunol.* **132**, 933–941 (2013).
- Seehus, C. R. et al. The development of innate lymphoid cells requires TOX-dependent generation of a common innate lymphoid cell progenitor. *Nat. Immunol.* **16**, 599–608 (2015).
- Zook, E. C. et al. The ETS1 transcription factor is required for the development and cytokine-induced expansion of ILC2. *J. Exp. Med.* **213**, 687–696 (2016).
- Halim, T. Y. F. et al. Retinoic-acid-receptor-related orphan nuclear receptor alpha is required for natural helper cell development and allergic inflammation. *Immunity* **37**, 463–474 (2012).
- Wong, S. H. et al. Transcription factor RORalpha is critical for nuocyte development. *Nat. Immunol.* **13**, 229–236 (2012).

33. Mohapatra, A. et al. Group 2 innate lymphoid cells utilize the IRF4-IL-9 module to coordinate epithelial cell maintenance of lung homeostasis. *Mucosal Immunol.* **9**, 275–286 (2016).
34. He, M. X. & He, Y. W. A role for c-FLIP(L) in the regulation of apoptosis, autophagy, and necroptosis in T lymphocytes. *Cell Death Differ.* **20**, 188–197 (2013).
35. Mandal, M. et al. The BCL2A1 gene as a pre-T cell receptor-induced regulator of thymocyte survival. *J. Exp. Med.* **201**, 603–614 (2005).
36. Ambrosini, G., Adida, C. & Altieri, D. C. A novel anti-apoptosis gene, survivin, expressed in cancer and lymphoma. *Nat. Med.* **3**, 917–921 (1997).
37. Marusawa, H. et al. HBXIP functions as a cofactor of survivin in apoptosis suppression. *EMBO J.* **22**, 2729–2740 (2003).
38. von Moltke, J. et al. Leukotrienes provide an NFAT-dependent signal that synergizes with IL-33 to activate ILC2s. *J. Exp. Med.* **214**, 27–37 (2017).
39. Lund, S. J. et al. Leukotriene C4 potentiates IL-33-induced Group 2 innate lymphoid cell activation and lung inflammation. *J. Immunol.* **199**, 1096 (2017).
40. Vivier, E. et al. Innate lymphoid cells: 10 years on. *Cell* **174**, 1054–1066 (2018).
41. Tait Wojno, E. D. & Artis, D. Emerging concepts and future challenges in innate lymphoid cell biology. *J. Exp. Med.* **213**, 2229–2248 (2016).
42. Doherty, T. A. & Broide, D. H. Lipid regulation of group 2 innate lymphoid cell function: Moving beyond epithelial cytokines. *J. Allergy Clin. Immunol.* **141**, 1587–1589 (2018).
43. Matsuda, A. et al. Generation of mice deficient in RNA-binding motif protein 3 (RBM3) and characterization of its role in innate immune responses and cell growth. *Biochem Biophys. Res Commun.* **411**, 7–13 (2011).
44. Zhu, X., Buhner, C. & Wellmann, S. Cold-inducible proteins CIRP and RBM3, a unique couple with activities far beyond the cold. *Cell Mol. Life Sci.* **73**, 3839–3859 (2016).
45. Kim, J. et al. Intratumorally establishing Type 2 innate lymphoid cells blocks tumor growth. *J. Immunol.* **196**, 2410–2423 (2016).
46. Colgan, S. P., Furuta, G. T. & Taylor, C. T. Hypoxia and Innate Immunity: Keeping Up with the HIFsters. *Annu Rev. Immunol.* **38**, 341–363 (2020).
47. Ushio, A. & Eto, K. RBM3 expression is upregulated by NF-kappaB p65 activity, protecting cells from apoptosis, during mild hypothermia. *J. Cell Biochem.* **119**, 5734–5749 (2018).
48. Gautier, V. et al. Extracellular IL-33 cytokine, but not endogenous nuclear IL-33, regulates protein expression in endothelial cells. *Sci. Rep.* **6**, 34255 (2016).
49. Petrova, T., Pesic, J., Pardali, K., Gaestel, M. & Arthur, J. S. C. p38 MAPK signalling regulates cytokine production in IL-33 stimulated Type 2 Innate Lymphoid cells. *Sci. Rep.* **10**, 3479 (2020).
50. Furusawa, J. et al. Critical role of p38 and GATA3 in natural helper cell function. *J. Immunol.* **191**, 1818–1826 (2013).
51. Yang, H. J. et al. RNA-binding protein RBM3 prevents NO-induced apoptosis in human neuroblastoma cells by modulating p38 signaling and miR-143. *Sci. Rep.* **7**, 41738 (2017).
52. Krabbendam, L., Bal, S. M., Spits, H. & Golebski, K. New insights into the function, development, and plasticity of type 2 innate lymphoid cells. *Immunol. Rev.* **286**, 74–85 (2018).
53. Zhang, K. et al. Cutting edge: notch signaling promotes the plasticity of Group-2 innate lymphoid cells. *J. Immunol.* **198**, 1798–1803 (2017).
54. Halim, T. Y. F. et al. Group 2 innate lymphoid cells are critical for the initiation of adaptive T helper 2 cell-mediated allergic lung inflammation. *Immunity* **40**, 425–435 (2014).
55. Gold, M. J. et al. Group 2 innate lymphoid cells facilitate sensitization to local, but not systemic, TH2-inducing allergen exposures. *J. Allergy Clin. Immunol.* **133**, 1142–1148 (2014).
56. Rajput, C. et al. RORalpha-dependent type 2 innate lymphoid cells are required and sufficient for mucous metaplasia in immature mice. *Am. J. Physiol. Lung Cell Mol. Physiol.* **312**, L983–L993 (2017).
57. Lund, S. J. et al. Leukotriene C4 potentiates IL-33-induced Group 2 innate lymphoid cell activation and lung inflammation. *J. Immunol.* **199**, 1096–1104 (2017).
58. Doherty, T. A. et al. Lung type 2 innate lymphoid cells express cysteinyl leukotriene receptor 1, which regulates TH2 cytokine production. *J. Allergy Clin. Immunol.* **132**, 205–213 (2013).
59. Zhou, B. et al. Thymic stromal lymphopoietin as a key initiator of allergic airway inflammation in mice. *Nat. Immunol.* **6**, 1047–1053 (2005).
60. Picelli, S. et al. Full-length RNA-seq from single cells using Smart-seq2. *Nat. Protoc.* **9**, 171–181 (2014).
61. Rosales, S. L. et al. A sensitive and integrated approach to profile messenger RNA from samples with low cell numbers. *Methods Mol. Biol.* **1799**, 275–301 (2018).
62. Pilotte, J., Cunningham, B. A., Edelman, G. M. & Vanderklish, P. W. Developmentally regulated expression of the cold-inducible RNA-binding motif protein 3 in eutherian rat brain. *Brain Res.* **1258**, 12–24 (2009).
63. Dresios, J. et al. Cold stress-induced protein Rbm3 binds 60S ribosomal subunits, alters microRNA levels, and enhances global protein synthesis. *Proc. Natl Acad. Sci. USA* **102**, 1865–1870 (2005).
64. Doherty, T. A. et al. Alternaria induces STAT6-dependent acute airway Eosinophilia and Epithelial FIZZ1 expression that promotes airway fibrosis and epithelial thickness. *J. Immunol.* **188**, 2622–2629 (2012).
65. Pilotte, J. et al. Morphoregulatory functions of the RNA-binding motif protein 3 in cell spreading, polarity and migration. *Sci. Rep.* **8**, 7367 (2018).

Acknowledgements

T.A.D. supported by NIH AI114585 and Veterans Affairs BLR&D BX005073. H.M.M. supported by NIH/NCI K99/ROO CA256526. We thank Dr. Amit Mehta and Samantha Rensch for assistance with qPCR studies.

Author contributions

T.D. and P.W.V. conceived of project and designed experiments. H.M.M. designed and performed experiments. J.H.B., A.N.S., L.L., B.C., K.C., Y.H., M.A., L.H.N., S.J.L., A.L., H.K., R.E.B., N.K., J.P. performed experiments. M.M. and G.S. performed and analyzed RNA-sequencing. J.H.B., T.D., H.M.M., P.W.V. analyzed data and wrote the manuscript.

Competing interests

The authors declare no competing interests.

Additional information

Supplementary information The online version contains supplementary material available at <https://doi.org/10.1038/s41467-022-32176-5>.

Correspondence and requests for materials should be addressed to Taylor A. Doherty.

Peer review information *Nature Communications* thanks Shigeo Koyasu and the other, anonymous, reviewer(s) for their contribution to the peer review of this work.

Reprints and permission information is available at <http://www.nature.com/reprints>

Publisher's note Springer Nature remains neutral with regard to jurisdictional claims in published maps and institutional affiliations.

Open Access This article is licensed under a Creative Commons Attribution 4.0 International License, which permits use, sharing, adaptation, distribution and reproduction in any medium or format, as long as you give appropriate credit to the original author(s) and the source, provide a link to the Creative Commons license, and indicate if changes were made. The images or other third party material in this article are included in the article's Creative Commons license, unless indicated otherwise in a credit line to the material. If material is not included in the article's Creative Commons license and your intended use is not permitted by statutory regulation or exceeds the permitted use, you will need to obtain permission directly from the copyright holder. To view a copy of this license, visit <http://creativecommons.org/licenses/by/4.0/>.

© The Author(s) 2022